

Production of strangeness -1 and -2 hypernuclei within a field theoretic model

R. Shyam

Saha Institute of Nuclear Physics, 1/AF Bidhan Nagar, Kolkata 700064, India

Abstract. We present an overview of a fully covariant formulation for describing the production of strangeness -1 and -2 hypernuclei using probes of different kinds. This theory is based on an effective Lagrangian picture and it focuses on production amplitudes that are described via creation, propagation and decay into relevant channel of intermediate baryonic resonance states in the initial collision of the projectile with one of the target nucleons. The bound state nucleon and hyperon wave functions are obtained by solving the Dirac equation with appropriate scalar and vector potentials. Specific examples are discussed for reactions which are of interest to current and future experiments on the hypernuclear production.

Keywords: strangeness -1 and -2 hyperon and hypernuclear production, Field theoretic model of (π^+, K^+) , (γ, K^+) and (K^-, K^+) reactions

PACS: 13.75.Jz, 21.80.+a, 14.20.pt, 25.80.Nv

INTRODUCTION

Hypernuclei represent the first kind of flavored nuclei (with new quantum numbers) in the direction of other exotic nuclear systems (e.g., charmed nuclei). They introduce a new dimension to the traditional world of atomic nuclei. With a new degrees of freedom (the strangeness), they provide a better opportunity to investigate the structure of atomic nuclei [1]. For example, since the hyperons do not suffer from the restrictions of the Pauli's exclusion principle, they can occupy all the states that are already filled up by the nucleons right upto the center of the nucleus. This makes them unique tools to investigate the structure of the deeply bound nuclear states (see, e.g., [2, 3]). The data on the hypernuclear spectroscopy have been used extensively to extract information about the hyperon-nucleon (YN) interaction within a variety of theoretical approaches [4, 5, 6].

Λ hypernuclei [they correspond to strangeness (S) -1] can be produced by beams of mesons, protons and also heavy ions. The electromagnetic probes like photons and electrons can also be used for this purpose. Although, the stopped as well as in-flight (K^-, π^-) [3, 7] and (π^+, K^+) [2, 3, 7] reactions have been most extensively used in the experimental investigations of their production, the feasibility of producing them via the (p, K^+) [8, 9, 10], (γ, K^+) [11, 12, 13] and $(e, e'K^+)$ [14, 15, 16, 17, 18, 19] reactions has also been demonstrated in the recent years. The (K^-, K^+) reaction is one of the most promising ways of studying the $S = -2$ Ξ hypernuclei because it leads to the transfer of two units of both charge and strangeness to the target nucleus. There is an experimental proposal approved at JPARC facility in Japan to produce such nuclei using this reaction.

Several features of various hypernuclear production

reactions can be understood by looking at the corresponding momentum transfers to the recoiling nucleus because it controls to some extent the population of the hypernuclear states. In Fig. 1, the momentum transferred to the recoiled nucleus is shown as a function of beam energy at two angles of the outgoing kaon for a number of reactions. We see that the (K^-, π^-) reaction allows only a small momentum transfer to the nucleus (at forward angles), thus there is a large probability of populating Λ -substitutional states in the residual hypernucleus (Λ occupies the same angular momentum state as that of the replaced neutron). On the other hand, in (π^+, K^+) , (γ, K^+) and (K^-, K^+) reactions the momentum transfers are larger than the nuclear Fermi momentum. Therefore, these reactions can populate hyperon states with configurations of a nucleon hole and a hyperon in a series of orbits covering all bound states. The momentum transfers involved in the (p, K^+) reaction are still larger by a factor of about 3. Thus, the states of the hypernuclei excited in the (p, K^+) reaction may have a different type of configuration as compared to those excited, e.g., in the (π^+, K^+) reaction. Nevertheless, it should be mentioned that usually larger momentum transfers are associated with smaller hypernuclear production cross sections. Each reaction has its own advantage and plays its own role in a complete understanding of the hypernuclear spectroscopy.

In this paper, we present a short review of the investigations made by us on the production of S -1 and -2 hypernuclei within an effective Lagrangian model [9, 10, 12, 13, 20, 21]. It retains the full field theoretic structure of the interaction vertices and treats baryons as Dirac particles. The initial state interaction of the incoming projectile with a free or bound target nucleon leads to excitation of intermediate baryon or hyperon resonant

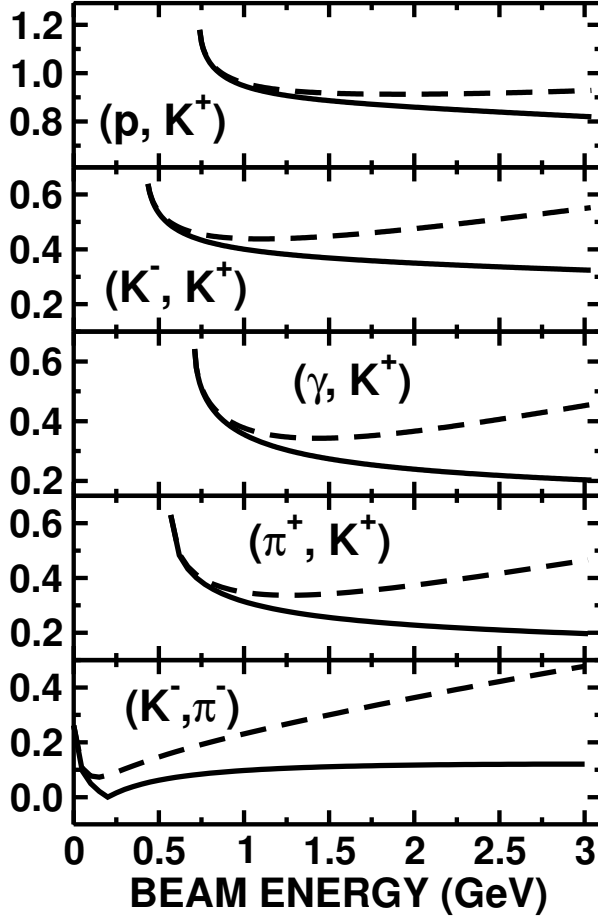


FIGURE 1. The momentum transfer involved in various hypernuclear production reactions as function of beam energy for the outgoing kaon angles of 0° (full lines) and 10° (dashed lines) for the ^{12}C target.

states, which propagate and subsequently decay into a K^+ meson and hyperon that gets captured into one of the nuclear orbits to produce the hypernucleus.

COVARIANT HYPERNUCLEAR PRODUCTION AMPLITUDES

Since we are still far way from calculating the intermediate energy scattering and reactions directly from the lattice QCD, the effective field theoretical description in terms of the baryonic and mesonic degrees of freedom is usually employed to describe these processes. These approaches introduce the baryonic resonance states explicitly in their framework and QCD is assumed to provide justification for the parameters or the cut-off functions used in calculations.

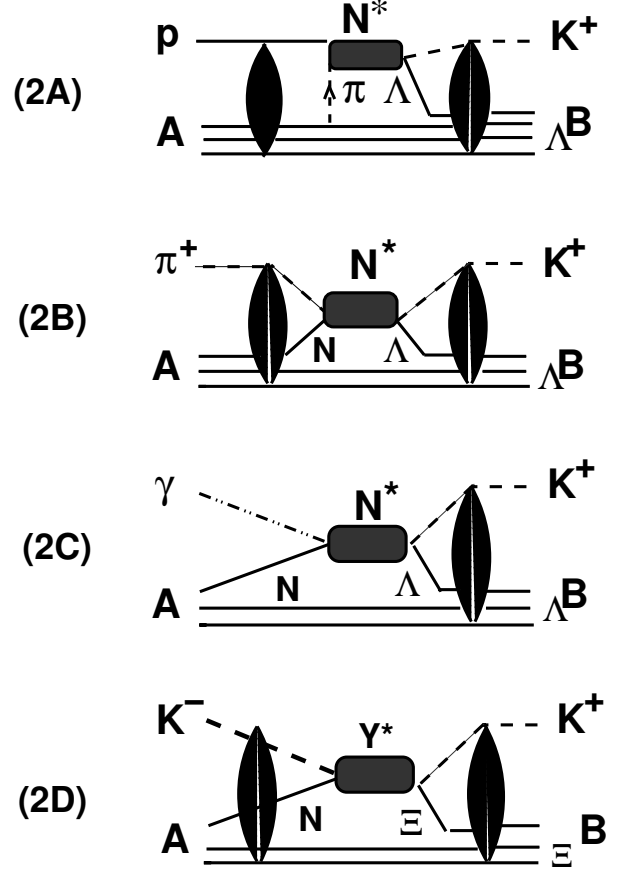


FIGURE 2. Types of the Feynman diagrams included in calculations of various reactions. In case of the (p, K^+) reaction another diagram also contributes to the total amplitude. This is known as the projectile emission diagram, where the exchanged pion emerges from the projectile vertex. The elliptic shaded areas represent the optical model interactions in the incoming or outgoing channels.

We use the diagrams shown in Fig. 2 for the calculations of the hypernuclear production reactions. In all the cases, the initial state interaction of the projectile with a bound nucleon of the target leads to excitations of intermediate resonance intermediate states that decay into kaon and the hyperon. The latter gets captured into one of the nuclear orbits. In case of reactions leading to the production of the Λ hypernuclei, we have included three nucleon resonances, $N^*(1650)[\frac{1}{2}^-]$, $N^*(1710)[\frac{1}{2}^+]$ $N^*(1720)[\frac{3}{2}^+]$, because they have appreciable branching ratios for decay into the $K^+\Lambda$ channel and are known to contribute predominantly to the corresponding elementary reactions involved in various processes [13, 22, 23]. On the other hand, in case of the (K^-, K^+) reaction leading to the production of Ξ hypernuclei, the intermediate channels are the hyperon states. We have considered the Λ , Σ hyperons and eight of their resonances with masses

up to 2.0 GeV [$\Lambda(1405)$, $\Lambda(1520)$, $\Lambda(1670)$, $\Lambda(1810)$, $\Lambda(1890)$, $\Sigma(1385)$, $\Sigma(1670)$, $\Sigma(1750)$], which are represented by Y^* in Fig. 2 (2D). These resonances have also been considered in a description of the Ξ hyperon production in the elementary $p(K^-, K^+)\Xi^-$ reaction within a similar model where a good description of the available total and differential cross sections has been obtained [24].

To calculate the amplitudes corresponding to the diagrams shown in Fig. 2, one requires the effective Lagrangians at the meson-baryon-resonance vertices (which involve coupling constants and the form factors), and the propagators for various resonances. They have been taken to be the same as those given Refs. [10, 13, 24, 21]. In addition, one needs spinors for the nucleon hole and hyperon particle bound states. They are obtained by following the procedure as discussed in the next section. In our model terms corresponding to the interference between various components of a given diagram are retained in the corresponding total production amplitude. Since calculations within this theory are carried out in the momentum space all along, they include all the nonlocalities in the production amplitude that arises from the resonance propagators.

RESULTS AND DISCUSSIONS

1. Hyperon bound state spinors

The spinors for the final hypernuclear bound state and for intermediate nucleonic states that are required for the calculations of various amplitudes, have been calculated within a phenomenological model where we assume these states to have pure-single particle or single-hole configurations. The hyperon bound states have been calculated in a phenomenological model where they are obtained by solving the Dirac equation with scalar and vector fields having a Woods-Saxon (WS) radial form. With a set of radius and diffuseness parameters, the depths of these fields are searched to reproduce the binding energy (BE) of a given state. Since the experimental values of the BEs for the Ξ^- bound states are as yet unknown, we have adopted the predictions of the latest version of the quark-meson coupling (QMC) model [25] for the corresponding BEs in our search procedure for these states. The spinors for the nucleon-hole states were also calculated in the same way. For a comprehensive discussion of these calculations we refer to, e.g., [21, 26]. In studies of the (γ, K^+) and (K^-, K^+) reactions in ref. [13] and [21], respectively, the spinors calculated within the latest version of the QMC model have also been used. The cross sections calculated by using these spinors are similar to those obtained with the phenomenological model

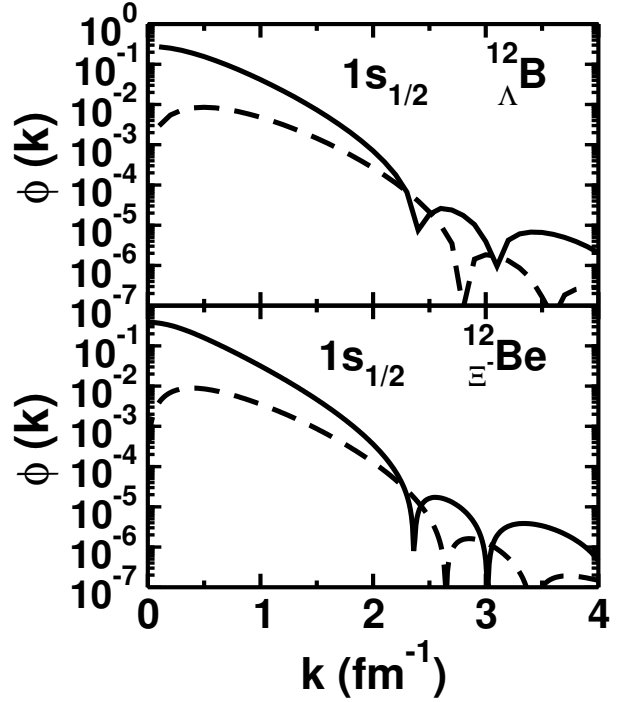


FIGURE 3. Magnitudes of the upper (full line) and lower (dashed line) components of the momentum space spinors for the hyperon orbit as shown.

The spinors in the momentum space are obtained by Fourier transformation of the corresponding coordinate space spinors.

In Fig. 3, we show the lower and upper components of the Dirac spinors in momentum space for the $0s_{1/2}$ Λ and Ξ^- hyperons in $^{12}_{\Lambda}\text{B}$ and $^{12}_{\Xi^-}\text{Be}$ hypernuclei that are generated, respectively, via the (γ, K^+) and (K^-, K^+) reactions on a ^{12}C target. The experimental BE of the Λ state is 11.37 MeV (see, e.g., Refs. [14, 16, 15]). Since the experimental values of the BE for the Ξ^- bound state is still unknown, we have adopted in our search procedure the corresponding value predicted in the latest version of the quark-meson coupling (QMC) model [25] which is 3.04 MeV [26]. With a radius and diffuseness parameters of 0.983 fm and 0.606 fm, the searched values of V_s and V_v are -212.70 MeV and 171.78 MeV, and -112.11 MeV and 90.81 MeV for the Λ and Ξ states, respectively. The values of $V_s + V_v$ that should be comparable to the depth of the corresponding conventional Woods-Saxon potentials, are -40.92 MeV and -21.30 MeV for Λ and Ξ interactions, respectively. Thus depth of the Ξ -nucleus interaction (V_{Ξ}) is about half of the Λ -nucleus interaction (V_{Λ}). Nevertheless, our V_{Ξ} is towards the higher side of the values available in the literature. While our potential is closer to that deduced in Ref. [27] (although their radius parameter was slightly bigger than ours), it is higher

than the shallow potential ($V_{\Xi} \approx -16$ MeV) conjectured from the emulsion events in the E176 experiment [28].

In each case, we note that only for momenta < 1.5 fm $^{-1}$, is the lower component of the spinor substantially smaller than the upper component. In the region of momentum transfer pertinent to the reactions under study, the lower components of the spinors are not negligible as compared to the upper component. This clearly demonstrates that a fully relativistic approach is essential for an accurate description of this reaction. In each case the momentum density of the hyperon shell, in the momentum region around 0.35 GeV/c, is at least 2-3 orders of magnitude larger than that around 1.0 GeV/c. Thus reactions involving lower momentum transfers are expected to have larger cross sections.

2. Production of Strangeness -1 hypernuclei

The Λ hypernuclei are the most studied $S = -1$ hypernuclear systems. They have been investigated using both hadronic (e.g., K^- , π) and electromagnetic (photon and electron) probes [2]. A comparison of relative merits of various probes of the production of Λ hypernuclei may be useful here. In contrast to the hadronic reactions e.g. [(K^-, π^-) and (π^+, K^+)], which take place mostly at the nuclear surface due to strong absorption of both K^- and π^\pm , the (γ, K^+) and $(e, e'K^+)$ reactions occur deep in the nuclear interior since K^+ -nucleus interaction is weaker. Thus, this reaction is an ideal tool for studying the deeply bound hypernuclear states if the corresponding production mechanism is reasonably well understood. While hadronic reactions excite predominantly the natural parity hypernuclear states, both unnatural and natural parity states are excited with comparable strengths in the electromagnetic reactions [29, 30, 31, 32]. This is due to the fact that sizable spin-flip amplitudes are present in the elementary photo-kaon production reaction, $p(\gamma, K^+)\Lambda$, since the photon has spin 1. This feature persists in the hypernuclear photo- and electro-production. Furthermore, since in these reactions a proton in the target nucleus is converted into a hyperon, it leads to the production of neutron rich hypernuclei (see, e.g., Ref. [33]), which may carry exotic features such as a halo structure. It can produce many mirror hypernuclear systems which would enable the study of the charge symmetry breaking with strangeness degrees of freedom. Our effective Lagrangian model has been used for describing the hypernuclear production using both the hadronic (p, K^+) [9, 10] and (π^+, K^+) [20], and the electromagnetic (γ, K^+) [13] reactions on a number of target nuclei. In the following we present some highlights of our calculations for the Λ hypernuclear production using the (γ, K^+) reaction.

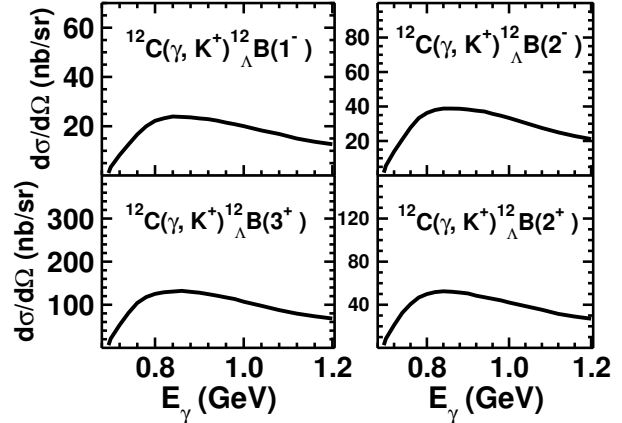


FIGURE 4. Differential cross sections (for the outgoing kaon angle of 10°) for the $^{12}\text{C}(p, K^+)^{12}_{\Lambda}\text{B}$ reaction leading to hypernuclear states as indicated.

2.1 Λ hypernuclear production via (γ, K^+) reaction

The threshold for the $^{12}\text{C}(\gamma, K^+)^{12}_{\Lambda}\text{B}$ reaction is about 695 MeV. The momentum transfer involved in this reaction at 10° kaon angles varies between approximately 2 fm $^{-1}$ to 1.4 fm $^{-1}$ for photon energies ranging between 0.7 GeV to 1.2 GeV [12]. In Fig. 4, we show the differential cross section at K^+ angle of 10° as a function of the photon energy (in the range 0.7-1.2 GeV) for this reaction. The hypernuclear states populated are 1^- , 2^- , and 2^+ , 3^+ corresponding to the particle-hole configurations of $(1p_{3/2}^-, 1s_{1/2}^{\Lambda})$ and $((1p_{3/2}^-, 1p_{3/2}^{\Lambda}))$, respectively. We note that within each configuration the highest J state is most strongly excited. Furthermore, unnatural parity states within each group are preferentially excited by this reaction. The unnatural parity states are excited through the spin flip process. Thus this confirms that kaon photo- and also electro-production reactions on nuclei are ideal tools for investigating the structure of unnatural parity hypernuclear states. The addition of unnatural parity states to the spectrum of hypernuclei is expected to constrain the spin dependent part of the effective $\Lambda - N$ interaction more tightly.

Another noteworthy aspect of Fig. 4 is that cross sections peak at photon energies around 850 MeV, which is about 200 MeV above the production threshold for this reaction. Interestingly, the total cross section of the elementary $p(\gamma, K^+)\Lambda$ reaction also peaks about the same energy above the corresponding production threshold (910 MeV). Therefore, the (γ, K^+) reaction on nuclei has the same basic features as that of the corresponding elementary reaction.

3. Production of Strangeness -2 hypernuclei

The (K^-, K^+) reaction provides one of the most promising ways of studying the $S = -2$ hypernuclei. This reaction implants a Ξ hyperon in the nucleus through the elementary $p(K^-, K^+)\Xi^-$ process. Therefore, it is essential to investigate first the (K^-, K^+) reaction on a proton target leading to the production of a free Ξ^- hyperon. This has been done in Ref. [24] within a similar effective Lagrangian model, where a good agreement has been achieved with available with experimental total and differential cross sections. The input information extracted from this study is then used in the description of the formation of Ξ^- -hypernuclei using this reaction.

3.1 Production of Ξ hypernuclei via (K^-, K^+) reaction

In this section, we discuss strangeness -2 hypernuclear production reactions $^{12}\text{C}(K^-, K^+)^{12}_{\Xi^-}\text{Be}$ and $^{28}\text{Si}(K^-, K^+)^{28}_{\Xi^-}\text{Mg}$. The threshold beam momenta for these reactions are about 0.761 GeV/c and 0.750 GeV/c, respectively. We have employed pure single-particle-single-hole ($p^{-1}\Xi$) configurations to describe the nuclear structure part. The QMC model predicts only one bound state for the $^{12}_{\Xi^-}\text{Be}$ hypernucleus with a binding energy of 3.038 MeV and quantum numbers $(1s_{1/2})$. On the other hand, for $^{28}_{\Xi^-}\text{Mg}$ it predicts 3 distinct bound Ξ^- states, $1s_{1/2}$, $1p_{3/2}$, $1p_{1/2}$, with corresponding binding energies of 8.982 MeV, 4.079 MeV, and 4.414 MeV, respectively [26]. These binding energies were used in our search procedure to obtain the spinors of the corresponding bound states.

In case of the ^{12}C target, the Ξ^- hyperon in a $1s_{1/2}$ state can populate 1^- and 2^- states of the hypernucleus corresponding to the particle-hole configuration $[(1p_{3/2})_p^{-1}, (1s_{1/2})_{\Xi^-}]$. The states populated for the $^{28}_{\Xi^-}\text{Mg}$ hypernucleus are $[2^+, 3^+]$, $[1^-, 2^-, 3^-, 4^-]$, and $[2^-, 3^-]$ corresponding to the configurations $[(1d_{5/2})_p^{-1}, (1s_{1/2})_{\Xi^-}]$, $[(1d_{5/2})_p^{-1}, (1p_{3/2})_{\Xi^-}]$, and $[(1d_{5/2})_p^{-1}, (1p_{1/2})_{\Xi^-}]$, respectively. In Fig. 5, we have shown results for populating the hypernuclear state with maximum spin of natural parity for each configuration. We have used a plane wave approximation to describe the relative motion of kaons in the incoming and outgoing channels. However, distortion effects are partially accounted for by introducing reduction factors to the cross sections as described in Ref. [34].

It is clear from Fig. 5 that for both the hypernuclear production reactions, the cross sections peak at p_{K^-} around 1.0 GeV/c which is ≈ 0.3 GeV/c above the production thresholds of the two reactions. It is not too different from the case of the elementary Ξ^- production

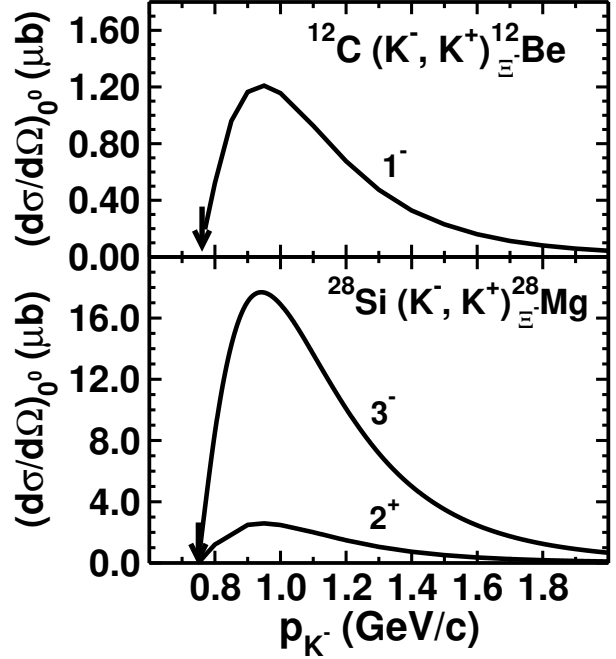


FIGURE 5. Differential cross section at 0° as a function of K^- beam momentum for the $^{12}\text{C}(K^-, K^+)^{12}_{\Xi^-}\text{Be}$ and $^{28}\text{Si}(K^-, K^+)^{28}_{\Xi^-}\text{Mg}$ reactions. The spin-parity of the final hypernuclear states are indicated on each curve.

cross sections where the peaks of the cross sections occur at about 0.35 -0.40 GeV/c above the corresponding production threshold (see Ref. [24]).

The magnitudes of the cross sections for the $^{12}_{\Xi^-}\text{Be}$ production are in excess of $1 \mu\text{b}$ near the peak position. It is important to note that at the beam momentum of 1.6 GeV/c, the magnitude of our cross section for this case is similar to that obtained in Ref. [34] within an impulse approximation model. Moreover, our cross sections at 1.8 GeV/c also are very close to those of Ref. [27] for both the targets. A more rigorous consideration of the distortion effects could alter the pattern of the beam momentum dependence, *e.g.* it is likely to be relatively stronger at lower values of p_{K^-} as compared to higher values. These effects will be investigated in a future publication.

4. SUMMARY AND CONCLUSIONS

In summary, it is clear that hypernuclear spectroscopy is indispensable for the quantitative understanding of the strangeness -1 and -2 hypernuclear structure and the hyperon-nucleon interaction. Driven by the new electron and kaon accelerator facilities, the field of hypernuclear production reactions is expected to experience a big boost. Already some data on the electron induced reac-

tions leading to the formation of Λ hypernuclei are available from the Jefferson Laboratory and more such data are expected to be available from the MAMI-C facility in the near future. Moreover, data on the strangeness -2 Ξ hypernuclei will soon be available from the JPARC facility in Japan. At the same time, our understanding of the hypernuclear production mechanism has improved significantly over the last decade.

A fully relativistic approach is essential for an accurate description of the hypernuclear production cross sections. It is feasible to calculate the reactions induced by hadronic and electromagnetic probes within a single fully covariant effective Lagrangian picture. Since the relevant elementary production cross sections are also described within the similar picture, most of the input parameters needed for the calculations of the hypernuclear production are fixed independently.

The feasibility of one such model has been investigated by us. It provides a good account of the available data on hypernuclear production via the (π^+, K^+) reaction on a number of target nuclei. It describes well the important features of the Λ and Ξ hypernuclear production cross sections via (γ, K^+) and (K^-, K^+) reactions, respectively. An important feature of our calculation is that in both the cases the production cross sections peak at projectile (γ or K^-) energies that are above the corresponding thresholds by almost the same amount as are the positions of the maxima away from their thresholds in the relevant elementary cross sections.

Some of the predictions of our model for the strangeness -2 hypernuclear production should be tested soon by experiments to be performed at the JPARC facility in Japan.

ACKNOWLEDGMENTS

The author wishes to acknowledge useful discussions with H. Lenske, U. Mosel, O. Scholten, A. W. Thomas, K. Tsushima.

REFERENCES

1. B. F. Gibson and E. V. Hungerford III, Phys. Rep. 257 (1995) 349.
2. O. Hashimoto, H. Tamura, Prog.Part.Nucl.Phys. 57 (2006) 564.
3. H. Bandō, T. Motoba and J. Žofka, Int. J. Mod. Phys. 5 2021 (1990) 2021.
4. E. Hiyama, M. Kamimura, T. Motoba, T. Yamada, and Y. Yamamoto, Phys. Rev. Lett. 85 (2000) 270.
5. C. M. Keil and H. Lenske, Phys. Rev. C 66 054307 (2002) 054307
6. N. Guleria, S. K. Dhiman, and R. Shyam, Nucl. Phys. A 886 (2012) 71
7. R. E. Chrien and C. B. Dover, Annu. Rev. Nucl. Part. Sci. 39 113 (1989).
8. J. Kingler et al., Nucl. Phys. A 634 (1998) 325.
9. R. Shyam, H. Lenske and U. Mosel, Phys. Rev. C 69 (2004) 065205.
10. R. Shyam, H. Lenske, and U. Mosel, Nuc. Phys. A 764 (2006) 313.
11. H. Yamazaki et al., Phys. Rev. C 52 (1995) 1157(R).
12. R. Shyam, H. Lenske, and U. Mosel, Phys. Rev. C 77 (2008) 052201 (R).
13. R. Shyam, K. Tsushima, and A. W. Thomas, Phys. Lett. B 676 (2009) 51.
14. T. Miyoshi et al., Phys. Rev. Lett. 90 (2003) 232502.
15. M. Iodice et al., Phys. Rev. Lett. 99 (2007) 052501.
16. L. Yuan et al., Phys. Rev. C 73 (2006) 044607.
17. F. Cusanno et al., Phys. Rev. Lett. 103 (2009) 202501.
18. P. Achenbach et al., Nucl. Phys. A 881 (2012) 187.
19. S. N. Nakamura et al., Phys. Rev. Lett. 110 (2013) 012502.
20. S. Bender, R. Shyam and H. Lenske, Nucl. Phys. A 839 (2010) 51.
21. R. Shyam, K. Tsushima and A. W. Thomas, Nucl. Phys. A 881 (2012) 255.
22. R. Shyam, Phys. Rev. C 60 (1999) 055213.
23. V. Shklyar, H. Lenske and U. Mosel, Phys. Rev. C 72 (2005) 015210.
24. R. Shyam, O. Scholten and A. W. Thomas, Phys. Rev. C 84 (2011) 042201(R).
25. P. A. M. Guichon, A. W. Thomas, and K. Tsushima, Nucl. Phys. A 814 (2008) 66.
26. K. Tsushima, R. Shyam and A. W. Thomas, arXiv:1209.1464 [Nucl-th].
27. C. B. Dover and A. Gal, Ann. Phys. 146 (1983) 309.
28. S. Aoki et al., Progr. Theo. Phys. 89 (1993) 493.
29. C. Bennhold and L.E. Wright, Phys. Rev. C 39 (1989) 927; *ibid* Phys. Lett. B191 (1987) 11.
30. T. Motoba, M. Sotona, and K. Itonaga, Progr. Theo. Phys. (suppl) 117 (1994) 123.
31. T.-S. H. Lee, Z.-Y. Ma, B. Saghai, and H. Toki, Phys. Rev. C 58 (1998) 1551.
32. F.X. Lee, T. Mart, C. Benhold, H. Haberzettl, and L. E. Wright, Nucl. Phys. A695 (2001) 237.
33. M. Agnello et al., Nucl. Phys. A 881 (2012) 322.
34. K. Ikeda, T. Fukuda, T. Motoba, M. Takahashi and Y. Yamamoto, Progr. Theo. Phys. 91 (1994) 747.